Probabilistic models of the role of oxygen in human decompression sickness

E. C. PARKER, S. S. SURVANSHI, P. B. MASSELL, AND P. K. WEATHERSBY
Naval Medical Research Institute, Bethesda, Maryland 20889-5607

Parker, E. C., S. S. Survanshi, P. B. Massell, and P. K. Weathersby. Probabilistic models of the role of oxygen in human decompression sickness. *J. Appl. Physiol.* 84(3): 1096–1102, 1998.—Probabilistic models of human decompression sickness (DCS) have been successful in describing DCS risk observed across a wide variety of N_2-O_2 dives but have failed to account for the observed DCS incidence in dives with high P_{O_2} during decompression. Our most successful previous model, calibrated with 3,322 N_2-O_2 dives, predicts only 40% of the observed incidence in dives with 100% O_2 breathing during decompression. We added 1,013 O_2 decompression dives to the calibration data. Fitting the prior model to this expanded data set resulted in only a modest improvement in DCS prediction of O_2 data. Therefore, two O_2-specific modifications were proposed: P_{O_2}-based alteration of inert gas kinetics (*model 1*) and P_{O_2} contribution to total inert gas (*model 2*). Both modifications statistically significantly improved the fit, and each predicts 90% of the observed DCS incidence in O_2 dives. The success of *models 1* and *2* in improving prediction of DCS occurrence suggests that elevated P_{O_2} levels contribute to DCS risk, although less than the equivalent amount of N_2. Both models allow rational optimization of O_2 use in accelerating decompression procedures.

oxygen effects; gas-exchange kinetics; risk function; hazard function

PROBABILISTIC MODELS of the risk of human decompression sickness (DCS) have been successful in describing the occurrence and even the time of occurrence of DCS (9, 13, 15, 17, 18). With rare exceptions (14, 19), only inert gases have been considered in such decompression modeling, on the assumption that the role of inert gases in the development of DCS is of overwhelming importance. In nearly all decompression models, inspired O_2 is treated as a "free" quantity and is not linked to the risk of DCS. O_2 is less available as a dissolved gas when it is bound to hemoglobin and when it is converted to the very soluble gas CO_2. That view is substantiated by measurements of tissue O_2 levels of only a few Torr under normoxic conditions (2).

The most successful probabilistic model has not performed well in predicting DCS risk in dives that use a high fraction (~100%) of O_2 in the breathing gas during decompression (9, 13), underpredicting the occurrence of DCS in these O_2 decompression dives by ~60%. In a subsequent prospective trial of O_2 decompression procedures, severe underprediction again occurred (11). These results contradicted the expectation of no O_2 effect found in a moderately large study of dives (19) with direct ascent after breathing mixtures with a P_{O_2} range of 0.2–1.3 atmospheres absolute (ata). The emphasis of the present study is to develop modifications to the previous model to identify a specific O_2 influence on the accumulation of DCS risk. The ideal modification would improve, or not disturb, the model's success with N_2-O_2 data while better describing the DCS outcomes observed in the O_2 decompression data. Such an improved model could then be applied to the practical optimization of the use of O_2 to accelerate decompression.

The O_2 effects explored here are of two very different forms, both based on observed physiology. In our first model a P_{O_2}-dependent alteration of the N_2 washin-washout kinetics acknowledges the pharmacological ability of P_{O_2} to alter central and peripheral circulation. Anderson et al. (1) demonstrated a progressive and significant reduction in cumulative N_2 excretion with increasing inspired O_2, although the difficult experimental procedure did not allow quantitative estimates of actual N_2 kinetic parameters. In our second model, some of the inspired O_2 is treated as an inert gas, adding to the tissue level of N_2 in leading to DCS risk. Hyperoxia is known to greatly increase P_{O_2} in tissues (2, 5), and some prior decompression studies concluded that O_2 was approaching N_2 in its DCS risk potency (3, 4, 8, 10). Tikuisis and Nishi (14) explored a bubble-based DCS risk model that included an explicit O_2 contribution, but they did not apply it to data as extensive as those used here, nor did they use it to predict time of DCS occurrence, which is the focus of the present study.

All our models are based on survival functions and are intended to predict the risk of occurrence of an undesirable outcome due to a risk-generating event, in this case the occurrence of DCS after a hyperbaric exposure. We construct a mathematical model that relates a small number of measured variables (time, pressure, gas mix) to a binary outcome (DCS: yes/no). Although we borrow from the terminology of physiology when we use a label such as "partial pressure of gas in tissue," we have made no direct physiological measurements. Gas terminology is used to aid visualization of a risk function. The success or failure of such a model rests strictly on its ability to predict the probability of occurrence of the outcome.

DATA

The data sets used in fitting models in this report were taken from carefully controlled and well-documented experimental dives conducted in the United States, Canada, and Great Britain, described in detail elsewhere (data sources are described in Ref. 16 with additional sources in Refs. 6 and 11). The basic data set (*group A* in Table 1) used in earlier model development (6, 9) contains 3,322 dives. The data set with ~100% O_2 breathed during decompression (*group B* in Table 1) contains 1,013 dives.

In the *group A* dives, there are 190 DCS and 110 marginal cases, giving an overall DCS incidence of 6.1%. (The APPENDIX lists the data by file names in the primary database of the Naval Medical Research Institute, which is available from the authors.) Marginal cases are mild events considered to be related to the hyperbaric exposure but not severe enough to warrant recompression treatment. These events are given a value of 0.1 DCS case on the basis of the experience of senior diving medical officers (9). Although the majority of dives in *group A* used compressed air (21% O_2), a large number of dives were performed with moderately enriched O_2 atmospheres. In most of these nonair dives a constant P_{O_2} of 0.7 ata was breathed, either throughout the dive or with interspersed periods of air breathing. Other nonair dives used a range of constant fraction of O_2 throughout the dive from 10 to 40%, resulting in P_{O_2} of 0.21–1.4 atmospheres absolute (ata) (19). None of the nonair dives used a significantly higher P_{O_2} during decompression than during the dive itself. The high P_{O_2} values (up to 4.0 ata) in the single-air category come from 58 short-duration (<3 min) dives from a submarine escape experiment, in which high pressures were present for <1 min. Without these 58 profiles, the upper limit of the P_{O_2} range for single-air dives would be 1.5 ata. Only two of the DCS cases in *group A* come from these escape dives.

Table 1. *Summary of data*

Type	Dives	Cases: DCS	Cases: Marginals	%DCS	P_{O_2}, ata	F_{O_2}
			Group A			
Single air	1,005	53	13	5.4	0.21–4.0*	0.21
Repetitive and multilevel air	565	34	15	6.3	0.21–1.3	0.21
Single nonair	678	25	18	4.0	0.19–1.5	0.10–0.70
Repetitive and multilevel nonair	607	26	3	4.3	0.21–1.2	0.21–0.70
Saturation	467	52	61	12.4	0.21–1.5	0.09–0.21
			Group B			
O_2 decompression	586	22	16	4.0	0.21– 2.8	0.21–0.99
O_2 surface decompression	427	11	1	2.6	0.21–2.6	0.21–0.98
Total	4,335	223	127	5.4		

DCS, decompression sickness; F_{O_2}, fraction of O_2; ata, atmospheres absolute. Marginal DCS = 0.1 DCS case (8). *In dives with >1.5 ata P_{O_2} in single air category, bottom time was <1 min.

Group B contains 33 DCS and 17 marginal cases, for an incidence of 3.4%. The dives in *group B* are of two types: *1*) air dives that use ~100% O_2 during decompression and *2*) air dives followed by ~100% O_2 during surface decompression procedures. Surface decompression involves omitting much of the usual decompression requirement, traveling quickly to the surface, and then recompression in a dry hyperbaric chamber, usually to a fixed pressure, after a brief interval at the surface. To allow for incomplete delivery of O_2 to the diver, we assume that immersed divers breathed 99.5% O_2 and dry divers 98% O_2. The consequences of choosing these particular values are discussed later. P_{O_2} within *group B* is 0.21–2.8 ata, with the majority of the O_2 exposures at 1.9 or 2.2 ata, corresponding to decompression stop depths of 30 and 40 feet of seawater.

The data include time of occurrence for all DCS cases and for many of the marginal cases. The time of symptom occurrence is represented in the data as an interval ($T_1 - T_2$) over which symptoms appeared, where T_1 is the latest time the diver was known to be entirely free of symptoms and T_2 is the time at which definite symptoms were first reported. The methods and rules of establishing $T_1 - T_2$ for most reported dives are described in detail elsewhere (16).

MODELS

The best-fitting model from our most recent N_2-O_2 modeling effort (9, 13) was used as the base model for this study (*model 0*). This model allows for exponential washin and a mixed exponential-linear washout of inert gas partial pressure (9, 12, 13). Risk accumulation for this model is characterized by an instantaneous risk (r) proportional to the sum of the risks of each of its three parallel compartments

$$\text{model 0: } r = \sum_{i=1}^{3} r_i = \sum_{i=1}^{3} A_i \left(\frac{\mathrm{Pti}_i + \mathrm{P_{met}} - \mathrm{P_{amb}} - \mathrm{Thr}_i}{\mathrm{P_{amb}}} \right); \quad r_i \geq 0 \tag{1}$$

where A_i is a scale factor and Pti_i is the inert (N_2) gas burden for the ith compartment. The inert gas burden represents all inert gas pressure in the compartment, including that in any bubbles present, as though it had remained in solution. P_{amb} is the ambient pressure, Thr_i is an estimated threshold parameter (9) for the ith compartment, and P_{met} is a small constant contribution of metabolic gases (venous P_{O_2} and P_{CO_2} and water vapor pressure), with a numerical value of 0.19 atmospheres. Pti_i is a function of the arterial inert gas partial pressure (Pa_{N_2}); a time constant (α_i), which conceptually represents blood perfusion to the tissue; and an estimated linear-exponential kinetic crossover

parameter (PXO_i)

$$\frac{dPti_i}{dt} = \frac{1}{\alpha_i}(Pa_{N_2} - Ps_{N_{2,i}}) \quad (2)$$

where Ps_{N_2} is the partial pressure of dissolved N_2 in the tissue.

If $Pti_i \leq (PXO_i + P_{amb} - P_{met})$, only dissolved gas is present and Pti_i equals Ps_{N_2} and gas exchange is simply exponential. If $Pti_i > (PXO_i + P_{amb} - P_{met})$, then a bubble is deemed to be present and excess gas comes out of solution, such that the Ps_{N_2} remains constant at a level of $(PXO_i + P_{amb} - P_{met})$. Thus, when depth and Pa_{N_2} are constant, exchange becomes linear with time. The parameters A_i, Thr_i, PXO_i, and α_i are estimated by fitting to the observed data.

Figure 1 illustrates the handling of inert gas partial pressure in *model 0* for a dive with O_2 decompression. In the hypothetical dive shown, two possible washout curves are plotted: one for a diver who breathes air (solid curve) throughout the decompression and another for a diver who breathes 100% O_2 (dashed curve) during a portion of the decompression. The duration of the O_2 period is indicated by the drop in Pa_{N_2} below that for breathing air. During the O_2 breathing period, N_2 washout accelerates because Pa_{N_2}, the asymptote (or forcing function) for the model's calculated N_2 partial pressure (Pti_{N_2}), is then essentially zero. Because *model 0* considers DCS risk to be proportional only to the area between the Pti_{N_2} curve and P_{amb}, risk is reduced, both in magnitude and duration, because of the O_2 breathing period. This risk reduction agrees qualitatively with the idea that breathing O_2 during decompression reduces the risk of DCS, but comparison of predictions with observed DCS incidence indicates that the reduction is too large (9, 13).

O_2-induced kinetic modifications. The first class of modification (*model 1*) changes the inert gas kinetic time constants for each compartment as a function of

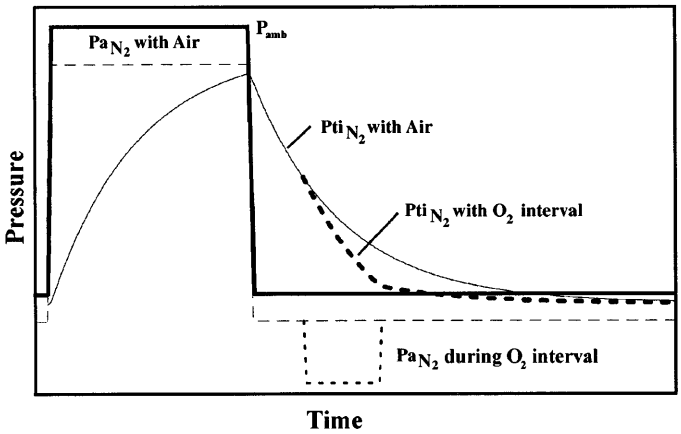

Fig. 1. *Model 0*: preferential washout of N_2 partial pressure in tissue (Pti_{N_2}) during O_2 breathing. Dashed line (Pa_{N_2} with air), arterial pressure of N_2 during air breathing; thin solid curve (Pti_{N_2} with air), model's washin-washout response; thick dashed line at *middle bottom* (Pa_{N_2} during O_2 interval), drop in N_2 pressure during 100% O_2 breathing; thick dashed curve (Pti_{N_2} during O_2 interval), model's response.

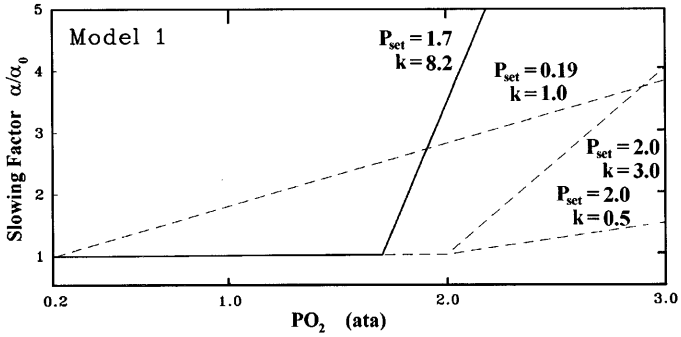

Fig. 2. *Model 1*: possible kinetic slowing effects as a function of P_{O_2}. Depending on values of estimated parameters P_{set} and k, *model 1* may produce a wide range of slowing factors. Solid line, slowing function resulting from best-fitting estimated parameter values.

inspired P_{O_2}. This type of modification is based on experimental results in which a reduction of whole body N_2 washout was observed with exposure to increasing P_{O_2} (1). This reduced N_2 washout is attributed to simultaneously observed reductions in cardiovascular parameters, including heart rate and blood flow. These combined effects can be modeled as O_2-induced reduction of perfusion rate, resulting in increased kinetic time constants. In *model 1* the modified time constant for each compartment is defined as

$$\textit{model 1: } \alpha_i = \alpha_{0,i} \cdot [1 + (P_{O_2} - P_{set_i}) \cdot k_i]; \quad (P_{O_2} - P_{set_i}) \geq 0 \quad (3)$$

where $\alpha_{0,i}$ is the unmodified inert gas time constant for the ith compartment (to be estimated by fitting to data), P_{O_2} is the inspired O_2 pressure, and P_{set} and k are parameters to be estimated from the data. P_{set} is a pressure threshold above which pressures of O_2 begin to cause kinetic slowing and k is simply a scale factor necessary to modulate the effect. There is no effect if P_{O_2} is less than P_{set}.

Figure 2 shows a range of effects for several values of P_{set} and k that *model 1* might have on an N_2 kinetic time constant over the P_{O_2} range contained in the data. The value on the *y*-axis is the exchange retardation factor $\alpha_i/\alpha_{0,i}$. It is clear from Fig. 2 that *model 1* can produce a wide range of subtle-to-pronounced effects, depending on the values of the parameters P_{set} and k. In particular, *model 1* is capable of yielding virtually no effect on α_0 for values of P_{O_2} generally observed in the air dives ($<$1.5 ata P_{O_2}) and an increasing effect for higher P_{O_2} levels. *Model 1* adds two estimated parameters per kinetic compartment, P_{set_i} and k_i, but some of the added parameters may not be warranted statistically and therefore may be dropped.

O_2 as an inert gas. In this model, O_2, at sufficiently high partial pressures, can contribute to bubble formation or growth (3–5, 8, 14). *Model 2* introduces the "O_2 effect" as a direct additive term in the supersaturation part of the risk function. Thus for the inert gas term in *Eq. 1*

$$\textit{model 2: } Pti_i = Pti_{N_{2,i}} + Pti_{O_{2,i}} \quad (4)$$

These burdens of N_2 and O_2 are governed by their own kinetic time constants. As in *model 0*, exponential and linear kinetics are possible. If $Pti_i \leq (P_{amb} + PXO_i - P_{met})$, then washout is exponential with independent N_2 and O_2 kinetics. However, if $Pti_i > (P_{amb} + PXO_i - P_{met})$, then the N_2 and O_2 washouts become linked, such that the sum of partial pressures of dissolved N_2 and O_2 remains constant at the level of $(P_{amb} + PXO_i - P_{met})$.

Not all the O_2 pressure will be considered to be available to contribute to DCS risk. We limit the contribution of O_2 to pressures above a certain level, P_{set_i}, to be estimated from the data, by controlling the effective O_2 pressure ($Peff_{O_2}$)

$$Peff_{O_2} = P_{O_2} - P_{set_i}; P_{O_2} > P_{set_i}$$
$$Peff_{O_2} = 0 \quad ; P_{O_2} \leq P_{set_i} \qquad (5)$$

A previous study (14) modeled the effect of O_2 with a similar parameterization, except the parameter P_{set} was applied asymmetrically. During O_2 uptake both constraints above were followed, whereas during O_2 washout negative values of $Peff_{O_2}$ were allowed, which leads to an accelerated washout of O_2. Under these conditions, P_{set} is required to simultaneously estimate the level at which O_2 is treated as an inert gas and the degree of enhanced O_2 washout after the dive, two potentially conflicting effects. Our P_{set} parameter estimates only the level of pressure above which O_2 is treated as an inert gas. *Model 2* adds two estimated parameters per kinetic compartment: P_{set_i} described above and $\alpha_{O_{2,i}}$ the exponential time constant for O_2 washin-washout.

Model evaluation. The risk functions, each model's set of equations leading to *Eq. 1*, were cast in standard risk (or hazard) function form to predict the probability of each observed dive in the data set and then into a likelihood (or log likelihood, LL) function. Details, especially those required to properly account for time of DCS onset, have been presented previously (17). Parameter estimation, propagation of errors, and formulation of likelihood ratio (LR) tests used standard methods, as in prior work (9, 15, 17, 18).

Each of the O_2 effect models is a modification of, and can be simplified to, *model 0*; therefore, an LR test (7, 18) is used to test for the significance of the added parameters contained in each modification. A proposed model will have a significantly improved fit to the data (at $P = 0.5$) if its LL exceeds the *model 0* LL (smaller negative number) by at least 1.92 for one added parameter and 2.98 for two added parameters, out to 6.30 for six added parameters (7). Each model was fitted to the combined data set ($A + B$). *Models 1* and *2* allow for up to six new parameters (2 per kinetic compartment) to be estimated, in addition to the kinetic time constants, scale factors, thresholds, and linear-exponential crossover parameters, which are common to all. Some or all of the added parameters may not add significantly to the improvement of the fit, as judged by the LR test. Final results for each model were chosen among many parameter estimation runs to include only those parameters the existence of which was justified at $P < 0.05$.

Results of fitting. Ideally, the O_2 effect parameters of any model would describe the data from *group B* in Table 1 and allow the basic parameters (those relating to *Eq. 1*) to better describe the data in *group A*. Table 2 lists the best-fit parameters and SEs estimated for each model.

The best fit of *model 1* improved LL by 11.1 units with only two additional estimated parameters, applied to *compartment 2*. The improvement is significant at $P < 0.01$. In *model 1*, estimated O_2 effect parameters result in no alteration of the N_2-based kinetics for <1.7 ata inspired P_{O_2}. A rapidly increasing effect was produced for higher values of P_{O_2}, up to an exchange retardation factor of ~10 (10 times slower gas kinetics) at 2.8 ata, the upper limit of P_{O_2} in the *group B* dives. The *model 1* effect curve for these estimated parameter values is shown in Fig. 2 (solid line). Additional O_2 effect parameters for *compartments 1* and *3* did not significantly improve LL.

The best fit of *model 2* improved the LL fit by 10.5 with two additional estimated parameters applied to *compartment 2*. This improvement is also significant at $P < 0.01$. The estimated N_2 time constant is substantially longer (slower) for *model 2* in *compartment 2* than for *model 0*. Although this slower time constant will result in less uptake of inert gas, it will also slow washout, thus allowing for longer risk accumulation for many dives. The specific O_2 effect parameters for this

Table 2. *Estimated parameters for models fitted to data A + B*

Parameter	Compartment 1	Compartment 2	Compartment 3	LL
		Model 0		
α	1.50 ± 0.71	32.5 ± 14.4	407.1 ± 19.0	1,200.1
A	3.6E-3 (2.7E-3)	4.5E-5 (2.1E-5)	1.0E-3 (1.2E-4)	
PXO		0.0 ± 0.03		
Thr			0.02 ± 0.01	
		Model 1		
α	1.61 ± 0.77	57.6 ± 16.0	508.4 ± 32.6	1,189.0
A	3.2E-3 (2.4E-3)	1.2E-4 (3.6E-5)	1.1E-3 (1.5E-4)	
PXO		0.03 ± 0.02		
Thr			0.07 ± 0.02	
P_{set}		1.69 ± 0.09		
k		8.23 ± 5.68		
		Model 2		
α	1.42 ± 0.75	85.8 ± 19.0	516.6 ± 43.9	1,189.6
A	3.4E-3 (2.7E-3)	1.8E-4 (5.1E-5)	9.4E-4 (1.4E-4)	
PXO		0.06 ± 0.02		
Thr			0.07 ± 0.02	
P_{set}		1.03 ± 0.23		
α_{O_2}		82.5 ± 67.8		

Values are estimated parameters ± SE; LL, log likelihood; α, nitrogen time constant (min); *A* and *k*, scale factors (dimensionless); PXO, linear-exponential kinetic crossover parameter (ata); Thr, threshold parameter (ata); P_{set}, O_2 pressure threshold (ata); α_{O_2}, oxygen time constant (min).

Table 3. *Prediction of DCS occurrence for models fit to data A + B*

Type	Observed DCS Cases	Predicted DCS Cases			
		Model 0	*Model 1*	*Model 2*	*Model 0A*
		Group A			
Single air	54.3	48.8 ± 7.2	45.8 ± 7.2	45.9 ± 7.5	44.5 ± 7.4
Repetitive and multilevel air	35.5	43.9 ± 5.9	40.7 ± 5.9	40.6 ± 6.3	39.9 ± 6.1
Single nonair	26.8	28.8 ± 4.3	26.4 ± 4.4	27.9 ± 4.2	25.7 ± 4.5
Repetitive and multilevel nonair	26.3	38.2 ± 5.0	32.0 ± 5.3	32.0 ± 7.6	31.1 ± 5.7
Saturation	58.1	52.8 ± 10.8	61.3 ± 13.9	60.1 ± 14.0	61.4 ± 14.1
Total	201.0	212 ± 27	206 ± 27	207 ± 27	203 ± 27
		Group B			
O_2 decompression	23.6	17.9 ± 3.4	19.4 ± 4.4	19.5 ± 4.6	9.9 ± 3.4
O_2 surface decompression	11.1	8.1 ± 2.0	12.2 ± 4.0	13.5 ± 4.7	3.8 ± 1.3
Total	34.7	26.0 ± 5.2	31.5 ± 8.1	31.2 ± 9.7	13.7 ± 4.4
Total	235.7	238 ± 30	237 ± 32	237 ± 30	216 ± 30

Values are model predictions ± 95% confidence level.

model apply a direct risk addition to *compartment 2* through the "combined" Pti_i (*Eq. 4*). This O_2-based contribution replaces overpressure "lost" due to the slower N_2 washin and applies this added risk specifically to the high-PO_2 segments only ($PO_2 > P_{set} = 1.03$ ata).

PREDICTION OF DCS

Table 3 lists the DCS occurrence predicted by each of the candidate models for the data used in fitting, along with the 95% confidence limits of each prediction obtained from propagation of errors. The last column in Table 3 gives predictions from *model 0* fit to *group A* only (*model 0A*). As expected, *model 0* predicts DCS in the combined data better than *model 0A* just by calibration to the combined *A + B* data. For example, the total DCS predicted by *model 0* increased to 238, from 216 predicted by *model 0A*, compared with 236 observed cases. This improvement is accomplished by increased prediction of DCS for all data types except saturation dives. However, *model 0* continues to underpredict DCS incidence in *group B* (by 25.1%) and fails to include the observed value within the 95% confidence limits of its prediction in *group B*, either as a whole or in its subsets.

It is clear from Table 3 that *models 1* and *2* have most of the desired predictive ability: prediction of DCS occurrence in *group A* dives centered nearly on the observed value and prediction of DCS occurrence in *group B*, which includes the observed value within its confidence limits. Also, *models 1* and *2* have maintained the quality of prediction of *model 0A* for dives in *group A*.

Tables similar to Table 3 can be used in χ^2 tests of "goodness of fit," where large values of the test statistic are taken as "failure" of the model to describe the distribution of the data. We can test each model's ability to predict DCS within each data group by separately considering the five categories of *group A* and two of *group B* from Table 3. The resulting *model 0, 1*, and *2* test statistics are 6.6, 2.9, and 3.3 for *group A* [4 degrees of freedom (df)] and 2.9, 1.0, and 1.3 for *group B* (1 df), respectively. None of these models "fails" to fit: all these χ^2 values yield $P > 0.05$. Similarly, we can break the 26 categories in the APPENDIX into the 21 belonging to *group A* and the 5 belonging to *group B*. The resulting *model 0*, *1*, and *2* test statistics are 23.3, 19.7, and 20.0 for *group A* and 11.8, 6.6, and 6.7 for *group B*. All *group A* tests yield $P > 0.05$ for 20 df. For *group B*, *model 0* has $P < 0.05$ and *models 1* and *2* have $P > 0.05$ for 4 df. This data categorization provides an indication that *model 0* does not predict DCS occurrence in the dives of *group B* as well as *models 1* and *2*. However, the outcomes of such χ^2 tests are clearly dependent on the choice of categorization. From results such as these and from many other instances where arbitrary but "reasonable" recategorization of data leads to "large" χ^2 statistics, we believe that such tests are only useful as a rough guide to identify problem areas. These areas can be identified more readily using line-by-line comparisons of observed and predicted results.

The inclusion of time of occurrence in our data allowed us to compare the predictive performance of the candidate models with the observed time distribution of DCS incidence. Figure 3 shows the observed and

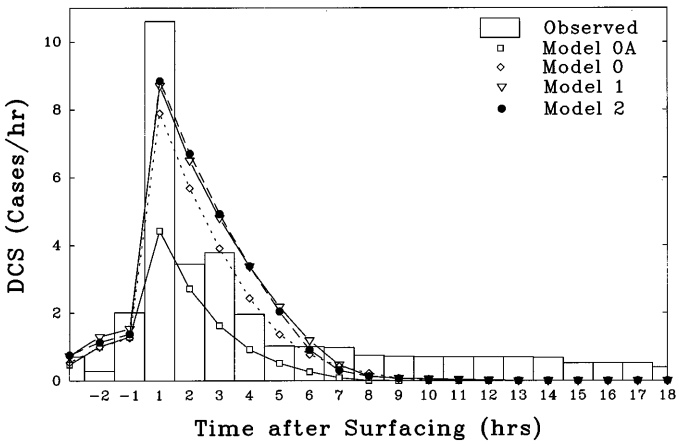

Fig. 3. Time of occurrence of decompression sickness (DCS). Predicted and observed DCS cases are shown for each hour after diver surfaces.

predicted DCS cases in each 1-h interval after surfacing for the dives in *group B*. Negative times indicate relatively rare events occurring during decompression before the divers reach the surface. *Model 0A* clearly underpredicts occurrence as a function of time throughout. *Model 0* shows substantial improvement over *model 0A*, with increased prediction for at least 8 h after the divers surface. *Models 1* and *2* have nearly identical predictions of occurrence in all time intervals but tend to overpredict in the 2- to 5-h range. Because almost one-third of the DCS cases are observed within the 1st h after surfacing, a good prediction here is particularly important. Here, the prediction of *model 2* (8.9 cases/h) comes closest to matching this value observed in the 1st h (10.6) but differs only slightly from that of *model 1* (8.7).

DISCUSSION

Both models of an O_2 contribution to DCS successfully described the expanded data set. Are the fully parameterized models plausible in light of the supposed underlying physiology? Because *model 1* was intended to incorporate the experimental observations of Anderson et al. (1), we compared the behavior of this model with those observations. They reported 9 and 17% reductions in the volume of whole body N_2 elimination compared with normoxic levels over 2 h of washout at 2.0 and 2.5 ata P_{O_2}, respectively. By use of the best-fit parameters shown in Table 2, the time constant for N_2 elimination in the second of three compartments in *model 1* was increased by factors of 2.55 and 6.67 at 2.0 and 2.5 ata P_{O_2}, respectively. A decrease in blood flow of >80% is large but not inconceivable. Over a 2-h washout period, these increased calculated time constants would result in 60 and 85% reductions, respectively, of the N_2 elimination expected from the unmodified time constant of 57.6 min, taking into account the asymmetric washout due to the mixed linear-exponential kinetics. It is reasonable to ignore the very fast and very slow compartments of the model compared with the experiment of Anderson et al. If *compartment 2* represents ~15–20% of the total N_2 gas volume, then the calculated reductions in N_2 elimination would translate approximately into the reported 9 and 17% whole body reductions.

Another human decompression study attempted to analyze N_2 exchange retardation from high O_2 pressures (19). Over the experimental range of 0.2–1.3 ata P_{O_2}, the single N_2 time constant did not appear to change, but parameter uncertainty allows the ~90-min time constant to slow to as much as ~130 min, which would represent an 18% reduction in N_2 elimination over a 2-h washout period.

Model 2 represents an approach fundamentally different from *model 1*, in that O_2, when present in pressures greater than P_{set_i} (Table 2), contributes directly to the risk generating overpressure, as defined in *Eqs. 1* and *4*. The estimated value of 1.03 ata for P_{set_2} requires that no O_2 effect on DCS risk be seen at pressures lower than this. This is a plausible threshold, in that O_2 levels in the tissue can be kept low until the hemoglobin dissociation curve is fully saturated above ~1.0 ata. A P_{set} of 1.03 ata allows for a contribution to DCS risk accumulation of 25–60% of the O_2 present during decompression in the dives of *group B*. This result is in general agreement with some animal studies (3, 4, 8, 10), which called for a 25–33% contribution from O_2. A prior human study (19) did not require an O_2 effect on risk but placed an upper bound of 40% contribution up to 1.3 ata P_{O_2} and thus is consistent with the present result. We note that combinations of *models 1* and *2*, incorporating a kinetic slowing and a direct contribution effect, were not successful in improving the fit relative to *model 1* or *model 2* as fit separately.

Our O_2 effect modifications were intended to remedy the failure of *model 0* to account for the DCS incidence observed in the O_2 data. Because our data coding of the inspired O_2 level in this data set is critical in all models, we should ask whether our data misrepresented the diver's actual gas exposure. In particular, we have explored the possibility that the coding of dry chamber O_2 decompressions, which form the bulk of *group B*, at 98% O_2 is incorrect because of imperfect delivery of the gas. Estimates from experienced investigators suggest that the minimum O_2 fraction likely to be present in the face mask in dry exposures is ~85–95% (R. Y. Nishi, personal communication). If the actual O_2 exposures were much less than our indicated 98%, *model 0*, without a specific O_2 contribution to DCS risk, might be able to account for the DCS incidence observation in *group B*. To explore this, *model 0* was calibrated to a series of altered data sets, with these dry O_2 exposures in *group B* modified to 60–90%. Only at ≤70% O_2 was *model 0* able to accurately predict the DCS outcome in *groups A* and *B*. With the data coded at ≥80%, the model's predictions were minimally changed from those shown for *model 0* in Table 3 (first "predicted" column). Thus our coding of the data at 98% does not directly "create" the need for an O_2 effect; even at a conservative value of 85%, *model 0* fails to describe the O_2 data. Similarly, inward skin flux of ambient N_2 from the air-filled chamber would increase the total body N_2 content but is unlikely to correspond to 20–30% of air breathing.

A third O_2 effect model added a fourth parallel risk compartment to *Eq. 1*, in which risk accumulation was based solely on P_{O_2} rather than on P_{N_2}. The best fit of this model improved the LL by only 3.8 (LL = 1196.3) with two additional estimated parameters: a time constant and a scale factor. Although this was a statistically significant improvement, it was not as impressive as those of *models 1* and *2*. This model's prediction of DCS incidence in *group A* was similar to that of *model 0*, and its prediction of DCS in *group B* (29.5 ± 6.9), although an improvement, was again less impressive than that of *model 1* or *model 2*. Its relatively poor fit and its problematic tie to plausible physiology led us to abandon the model.

The present results suggest that use of O_2 much over 1 ata has drawbacks that warrant consideration in optimizing decompression. This does not mean that O_2

is not useful during decompression, only that O_2 is not totally free of concern for causing DCS. Either of the two new models can be used for O_2 decompression optimization.

APPENDIX

Individual data set observed and predicted DCS cases

	Observed DCS	Predicted DCS			
		Model 0	*Model 1*	*Model 2*	*Model 0A*
		Group A			
Single air					
EDU885A	30.0	28.2	27.5	27.7	26.6
DC4W	8.4	5.7	5.7	5.5	5.6
SUBX87	2.0	0.6	0.5	0.5	0.5
NMRNSW	5.5	6.1	5.3	5.6	5.2
PASA	5.2	3.4	2.8	2.6	2.7
NSM6HR	3.2	4.9	4.0	4.1	3.9
Repetitive and multi-level air					
EDU885AR	11.0	11.7	12.0	11.8	11.7
DC4WR	3.0	1.0	1.0	1.0	0.9
PARA	7.3	10.5	9.8	9.6	9.6
PAMLA	14.2	20.6	18.1	18.3	17.6
Single nonair					
NMR8697	12.8	17.0	15.4	16.4	15.1
EDU885M	4.0	3.8	3.5	3.5	3.4
EDU1180S	10.0	7.9	7.5	8.1	7.3
Repetitive and multi-level nonair					
EDU184	11.0	15.6	14.3	14.7	13.9
PAMLAOD	6.0	9.8	7.6	7.1	7.3
PAMLAOS	5.3	7.9	6.1	6.0	5.9
EDU885S	4.0	4.9	4.1	4.2	3.9
Saturation					
ASATEDU	15.7	12.9	15.0	14.4	15.0
ASATNMR	1.0	4.6	4.6	4.1	4.5
ASATNSM	20.1	17.8	22.5	22.6	22.7
ASATARE	21.3	17.5	19.2	18.9	19.2
		Group B			
O_2 decompression					
DC8AOW	3.1	0.7	0.9	1.0	0.4
DC8AOD	3.2	3.5	3.2	4.5	1.6
NMR94EOD	17.3	13.7	15.2	14.0	7.9
O_2 surface decompression					
DC8ASUR	10.1	6.3	9.8	9.1	2.9
DCSUREP	1.0	1.8	2.5	2.6	0.9

We are indebted to several colleagues for their advice and guidance: R. Y. Nishi for consultation on modeling and data collection; P. Tikuisis, E. D. Thalmann, and L. D. Homer for insights on physiology and modeling; A. L. Harabin for several critical reviews through which the manuscript was much improved; and S. Mannix for valuable editorial assistance.

This work was supported by Naval Medical Research and Development Command Work Unit 0603713N M0099.01A-1510.

The opinions and assertions contained herein are the private ones of the authors and are not to be construed as official or reflecting the views of the Navy Department or the naval service at large.

Address for reprint requests: E. C. Parker, Albert R. Behnke Diving Medicine Research Center, Naval Medical Research Institute, 8901 Wisconsin Ave., Bethesda, MD 20889-5607.

Received 10 February 1997; accepted in final form 3 November 1997.

REFERENCES

1. **Anderson, D., G. Nagasawa, W. Norfleet, A. Olszowka, and C. Lundgren.** O_2 pressures between 0.12 and 2.5 atm abs, circulatory function and N_2 elimination. *Undersea Biomed. Res.* 18: 279–292, 1991.
2. **Clark, A., P. A. A. Clark, R. J. Connett, T. E. Gayeski, and C. R. Honig.** How large is the drop in P_{O_2} between cytosol and mitochondrion? *Am. J. Physiol.* 252 (*Cell Physiol.* 21): C583–C587, 1987.
3. **Donald, K. W.** Oxygen bends. *J. Appl. Physiol.* 7: 639–644, 1955.
4. **Eaton, W. J., and H. V. Hempleman.** *The Role of Oxygen in the Aetiology of Acute Decompression Sickness.* Alverstoke, UK: Royal Navy Physiology Laboratory, 1973. (Rep. 12-73)
5. **Jamieson, D., and H. A. S. VanDenBrenk.** Measurement of oxygen tensions in cerebral tissues of rats exposed to high pressures of oxygen. *J. Appl. Physiol.* 18: 869–876, 1963.
6. **Kelleher, P. C., E. D. Thalmann, S. S. Survanshi, and P. K. Weathersby.** Verification trial of a probabilistic decompression model (Abstract). *Undersea Biomed. Res.* 19, *Suppl.*: 78, 1992.
7. **Kendall, M. G., and A. Stewart.** *The Advanced Theory of Statistics* (4th ed.). London: Hafner, 1979, vol. 2, p. 38–180.
8. **Lillo, R. S.** Effect of N_2-He-O_2 on decompression outcome in rats after variable time-at-depth dives. *J. Appl. Physiol.* 64: 2042–2052, 1988.
9. **Parker, E. C., S. S. Survanshi, P. K. Weathersby, and E. D. Thalmann.** *Statistically Based Decompression Tables. VIII. Linear-Exponential Kinetics.* Bethesda, MD: Naval Medical Research Institute, 1992. (NMRI Rep. 92-73)
10. **Rashbass, C., and W. J. Eaton.** *The Effect of Oxygen Concentration on the Occurrence of Decompression Sickness.* Alverstoke, UK: Royal Navy Physiology Laboratory, 1957. (Rep. 10-57)
11. **Survanshi, S. S., E. D. Thalmann, E. C. Parker, D. D. Gummin, A. S. Isakov, and L. D. Homer.** *Dry Decompression Procedure Using Oxygen for USN Special Operations.* Bethesda, MD: Naval Medical Research Institute, 1997. (NMRI Rep. 97-03)
12. **Thalmann, E. D.** *Phase II Testing of Decompression Algorithms for Use in the US Navy Underwater Decompression Computer.* Panama City, FL: Navy Experimental Diving Unit, 1984. (NEDU Rep. 1-84)
13. **Thalmann, E. D., E. C. Parker, S. S. Survanshi, and P. K. Weathersby.** Improved probabilistic decompression model risk predictions using linear-exponential kinetics. *Undersea Hyperb. Med.* 18: 255–274, 1997.
14. **Tikuisis, P., and R. Y. Nishi.** *Role of Oxygen in a Bubble Model for Predicting Decompression Illness.* Toronto, ON, Canada: Defence and Civil Institute of Environmental Medicine, 1994. (DCIEM Rep. 94-04)
15. **Tikuisis, P., P. K. Weathersby, and R. Y. Nishi.** Maximum likelihood analysis of air and HeO_2 dives. *Aviat. Space Environ. Med.* 62: 425–431, 1991.
16. **Weathersby, P. K., B. L. Hart, E. T. Flynn, and W. F. Walker.** Role of oxygen in the production of human decompression sickness. *J. Appl. Physiol.* 63: 2380–2387, 1987.
17. **Weathersby, P. K., S. S. Survanshi, L. D. Homer, E. C. Parker, and E. D. Thalmann.** Predicting the time of occurrence of decompression sickness. *J. Appl. Physiol.* 72: 1541–1548, 1992.
18. **Weathersby, P. K., S. S. Survanshi, and R. Y. Nishi.** Relative decompression risk of dry and wet chamber air dives. *Undersea Biomed. Res.* 17: 333–352, 1990.
19. **Weathersby, P. K., S. S. Survanshi, R. Y. Nishi, and E. D. Thalmann.** *Statistically Based Decompression Tables. VII. Primary Data for Testing Human N_2O_2 Decompression Models.* Groton, CT: Naval Submarine Medical Research Laboratory, 1992. (Rep. 1182 and NMRI Rep. 92-85)